

Supporting Information

Coupling Protein Dynamics with Enzyme Catalysis in Human Carbonic Anhydrase II

Srabani Taraphder^{†,*}, C. Mark Maupin[‡], Jessica M. J. Swanson[§] and Gregory A. Voth^{§,*}

[†]Department of Chemistry, Indian Institute of Technology, Kharagpur 721302, India

[‡]Department of Chemical and Biological Engineering, Colorado School of Mines, 1500 Illinois Street, Golden, CO 80401

[§]Department of Chemistry, James Frank Institute, and Computation Institute, University of Chicago, 5735 South Ellis Avenue, Chicago, Illinois 60637

Free energy barriers for His64 rotation and proton transport from earlier simulation studies

Classical MD simulation studies¹⁻² reporting the potential-of-mean force (PMF) for the His64 rotation have shown that it prefers the inward conformation prior to dissociation of the proton from the zinc-bound water, and the outward conformation when His64 is protonated. The estimated free energy barrier of 5.6 kcal·mol⁻¹ is large when compared to thermal fluctuations, making the conformational transition a rare event at physiological temperatures.¹ However, the His64 sidechain re-orientation barrier is small when compared to the barrier of the rate limiting PT event, ~10 to 11 kcal·mol⁻¹, indicating that the sidechain re-orientation is fast when compared to the timescale of the catalyzed reaction.

Table S1 Estimated free energy change (ΔF) and free energy barrier (F^\ddagger) for sidechain conformational transitions in human carbonic anhydrase II (HCA II) from **classical** MD simulation with umbrella sampling.

Conformational transition	ΔF (kcal mol ⁻¹)	F^\ddagger (kcal mol ⁻¹)
EZn-H ₂ O ²⁺ -His64 (in) → EZn-H ₂ O ²⁺ -His64 (out)	1.6	5.6
EZn-OH ⁺ -His64.H ⁺ (out) → EZn-OH ⁺ -His64.H ⁺ (in)	3.2	6.2

Table S2 Estimated potential of mean force (PMF) barrier, F^\ddagger for the deprotonation of zinc-bound water molecule followed by proton transfer (PT) to His64 sidechain with different orientations in human carbonic anhydrase II (HCA II) using multi-state empirical valence bond (MS-EVB) method

System	Description	F^\ddagger (kcal mol ⁻¹)
1	His64 in its inward orientation and included in the MS-EVB basis set	10.0 ± 0.4
2	His64 in its outward orientation and excluded from the MS-EVB basis set	14.6 ± 0.4
3	His64 in its outward orientation and included the MS-EVB basis set	11.4 ± 0.4

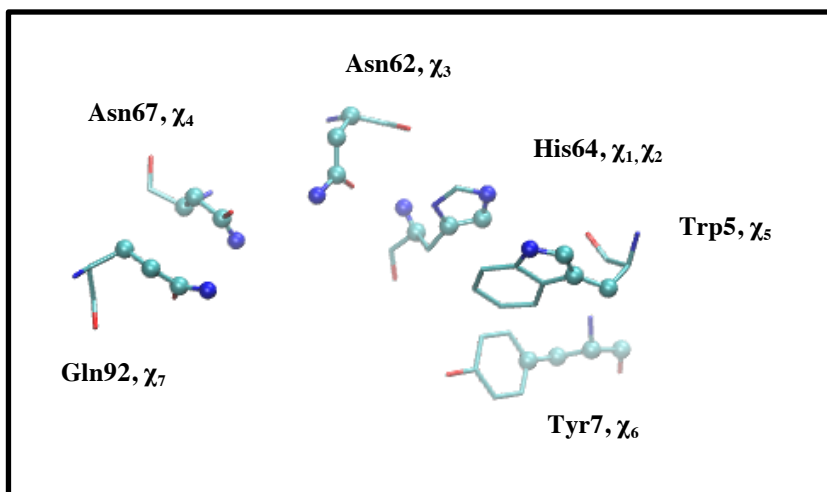
Benchmarking studies on the transition path ensemble.

There are several important issues that need close inspection in order to correctly sample the transition path ensemble. The number of studies reported in the literature combining a hybrid QM-MM description of the reaction to a rare event sampling method such as TPS is essentially limited on account of the large scale computational resources that are required and the technical difficulty involved.³⁻⁷ Therefore, it is of primary importance to establish the statistical significance of the ensemble of a limited number of trajectories before one proceeds further.

For system 1 (forward flux transition path sampling) the sampling time of 1 ps was appropriate given that the residence time τ_b was negligible due to the rapid movement of the CEC, on the fs time scale, to the His64 residue, and the fact that re-crossing was rarely observed. For the slower PT event in systems 2 and 3 (with ensembles of full dynamical transition paths), the length of each trajectory has been restricted to 10 ps. This choice of simulation time is justified based on the residence time, τ_b , that is defined as the time interval spent by a given reactive trajectory between its first entry into and last exit from the barrier region. The calculated residence time for the ensemble of trajectories generated yielded an average value of $\tau_b = 6 \pm 3$ ps with a distribution of τ_b that contains a substantial number of residence times ~ 9 ps. To evaluate systems with relatively long residence times trajectories with a τ_b greater than 9 ps were selected and simulated for up to 15 ps to examine if any new mechanisms were viable for these particular trajectories. However, no new mechanism was found for these longer runs.

Another aspect of ensuring computational efficiency involves determination of an optimum number of reactive trajectories in the ensemble such that the dynamics of the complex system are adequately sampled. The optimization of the reactive trajectory ensemble requires detailed information of the system when occupying the barrier region, which was available from previous simulations that evaluated the PMF for the rate limiting PT event.⁸ The biased umbrella sampling used to generate the PMF provided ~ 1 ns of simulation data for the barrier top region in the constant NVT ensemble, which was used to ensure that the reactive trajectory ensemble adequately sampled the system dynamics. A detailed comparison between the biased trajectories and the reactive trajectories was conducted that included properties such as the root-mean-squared deviation, spatial occupancy analysis of the CEC and active site water molecules, and the mass-weighted correlation matrix. Comparison of the two sets of results indicated no significant difference and was therefore concluded to adequately describe the behavior at the barrier top in spite of the restricted number of simulations and time span (data not shown).

Figure S1 Important sidechain dihedral angles of active site residues as defined in Table 2 of the main text. Contributing atoms of each dihedral angle are highlighted using spheres.



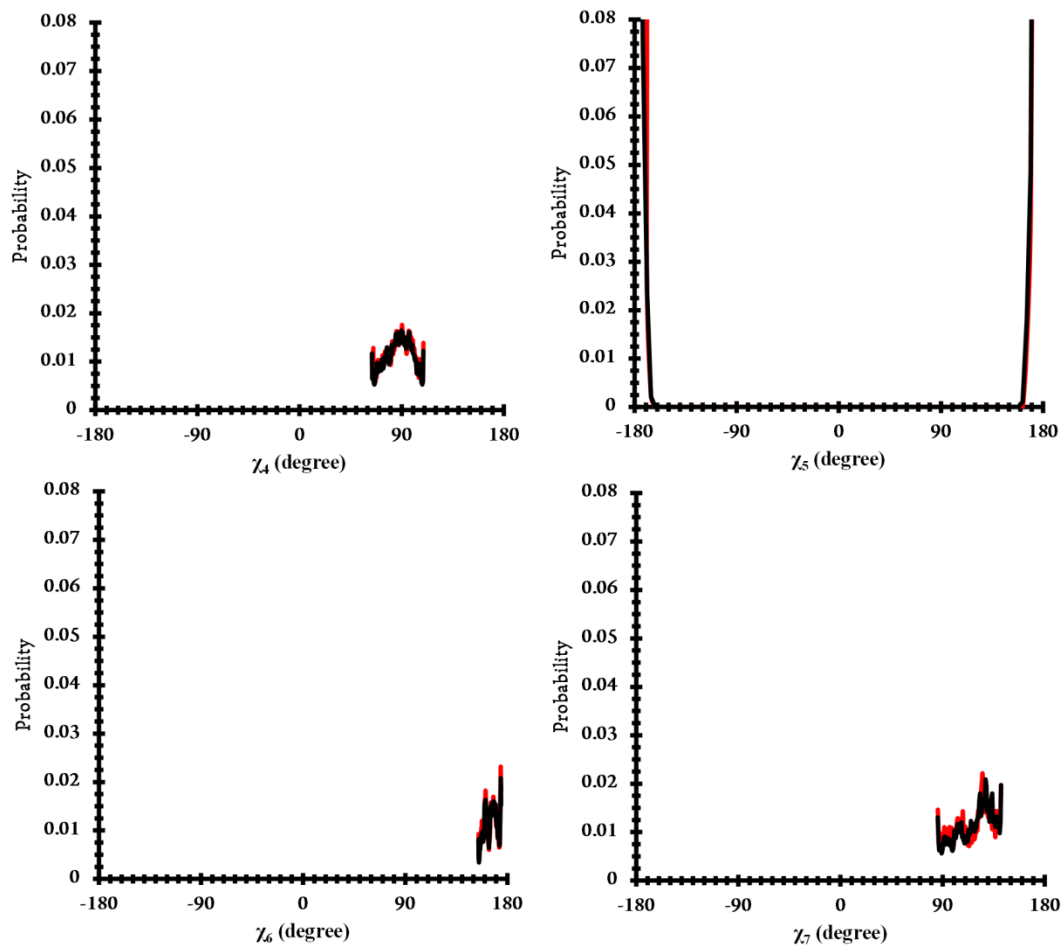


Figure S2 Distribution of key sidechain dihedral angles when His64 is present in its inward orientation for transition paths with $\tau_{\text{txn}} \leq 50$ fs (black) and when the excess proton resides on the His64 sidechain (red). The black and red lines for χ_2 are depicted by dotted lines for clarity.

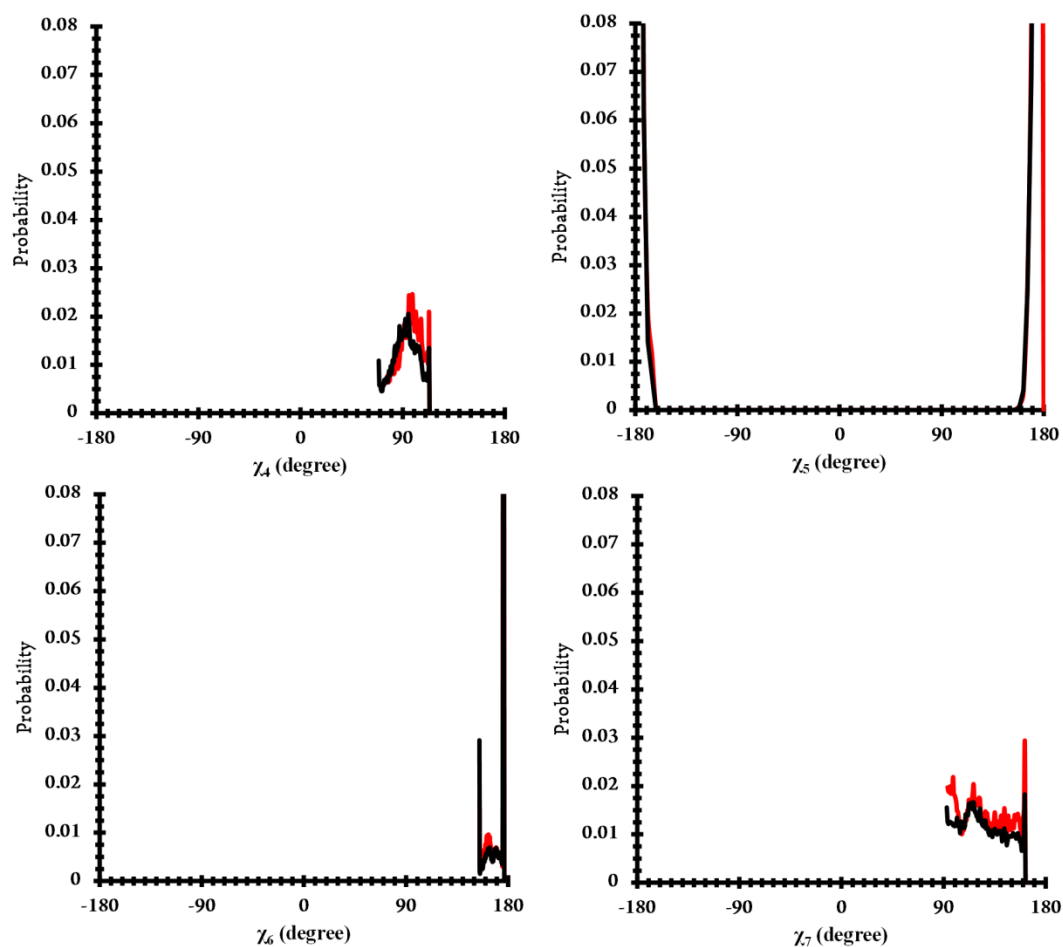


Figure S3 Distribution of key sidechain dihedral angles when His64 is present in its inward orientation for transition paths with $50 < \tau_{\text{rxn}} \leq 250$ (fs) (black) and when the excess proton resides on the His64 sidechain (red). The black and red lines for χ_2 are depicted by dotted lines for clarity.

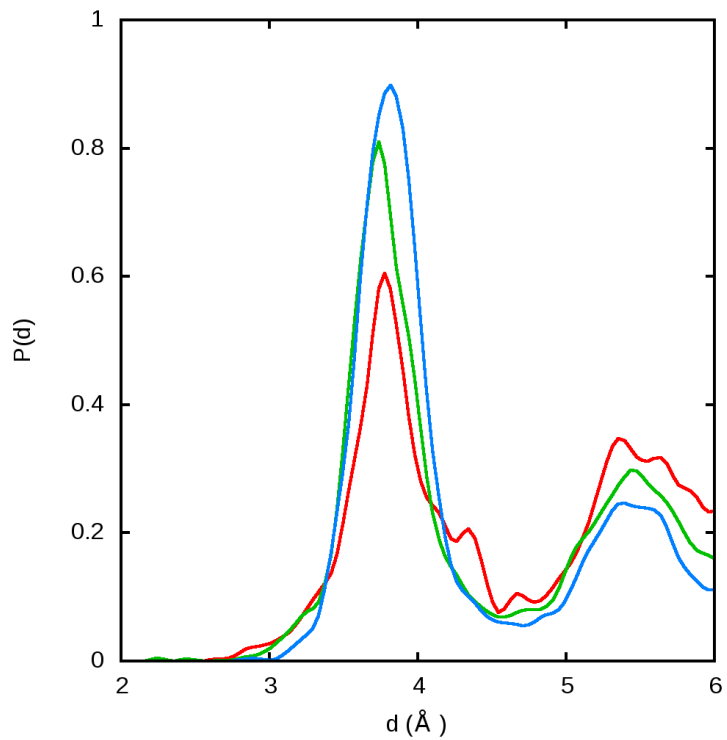


Figure S4 Average distribution, $P(d)$, of water molecules at a distance $d \leq 6.6 \text{ \AA}$ from the zinc ion at the active site cavity for the transition paths belonging to group A (red), C (green) and E (blue) when His64 is in its *out* orientation and *excluded* from proton relay.

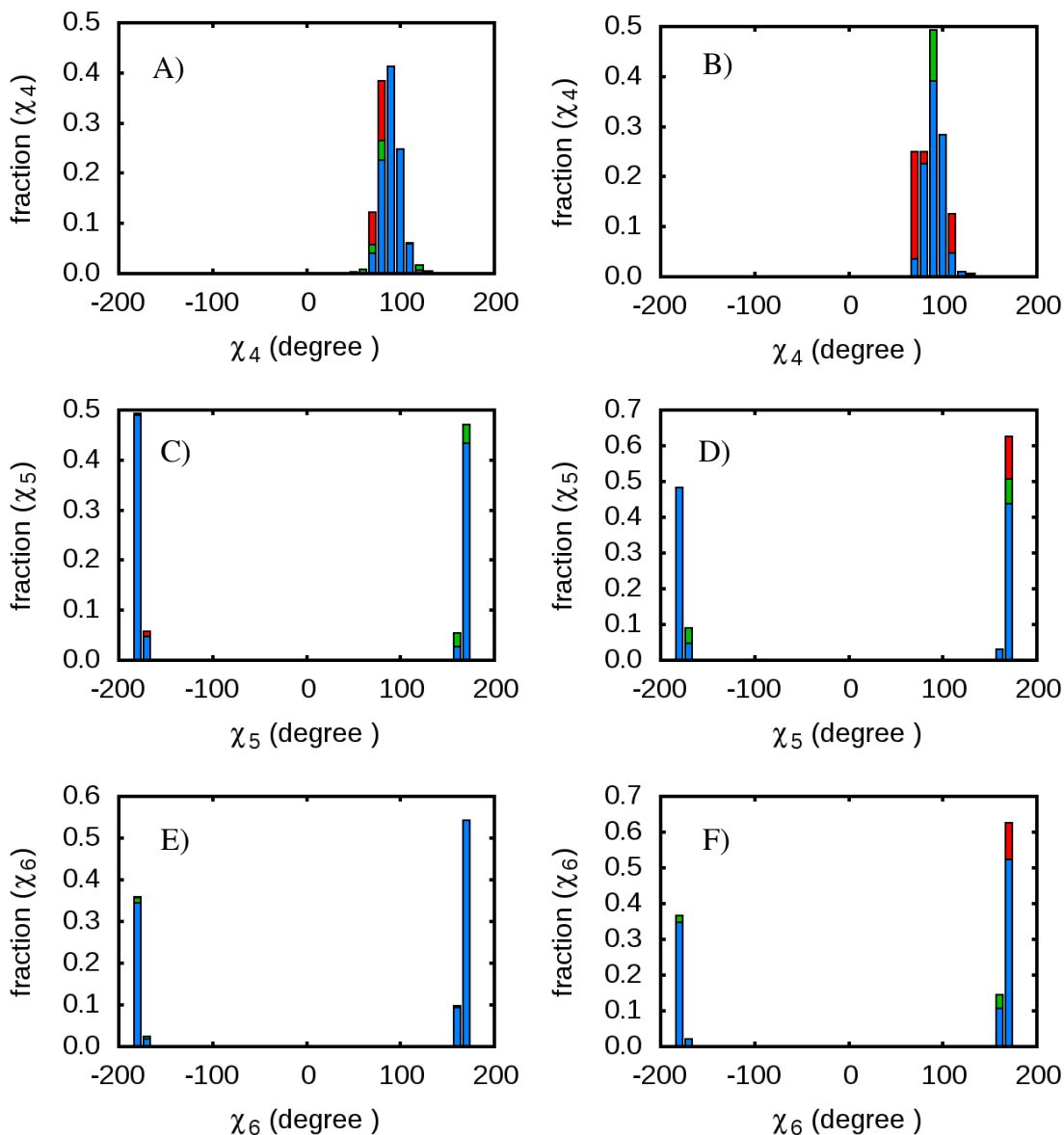


Figure S5 Distribution of sidechain dihedral angles χ_4 (A,B), χ_5 (C,D) and χ_6 (E,F) (as defined in Table 2) for the transition paths belonging to group A (red), C (green) and E (blue) when His64 is in its *out* orientation and *excluded* from proton relay. The distributions on the left (A,C,E) represent the entire transition path while those on the right (B,D,F) are only from the barrier segment.

Dynamics of key active site dihedral angles

System 1

As explained in the main article, a short, 10 fs long segment is chosen from each transition path harvested within System 1 centered around $t = \tau_{rxn}$. For N paths, the percentage change in each dihedral angle, χ_i ($i=1,7$) around τ_{rxn} is then computed as follows.

$$\Delta\chi_i = \frac{100}{\chi_i(crystal)} \frac{1}{N} \sum_{i=1}^N \frac{1}{n_i} \sum_{j=1}^{n_i} [\chi_i(j) - \chi_i(crystal)]$$

In the above expression, the averaging is carried out over N 10-fs segments. The i -th segment is assumed to have n_i time slices. At each of these time slices, the change in χ_i with respect to its crystallographic value $\chi_i(crystal)$ is calculated. The resultant data are shown below.

Table S2 The percentage change, $\Delta\chi$ of important active site dihedral angles obtained by averaging over the 10 fs segments extracted from ultrafast ($\tau_{rxn} \leq 50$ fs) and fast (50 fs $<$ $\tau_{rxn} \leq 250$ fs) proton transfer paths in System 1.

Group	$\Delta\chi_1$	$\Delta\chi_2$	$\Delta\chi_3$	$\Delta\chi_4$	$\Delta\chi_5$	$\Delta\chi_6$	$\Delta\chi_7$
Ultrafast	-51.9	-167.8	-72.7	-967.7	-66.7	-133.7	-137.1
Fast	-82.9	-100.3	-99.8	174.1	-106.5	-97.9	-94.0

The data presented above, along with those in Supporting Information Figures 1 and 2 emphasize the importance of *transient* reorganization of χ_4 - χ_7 in assisting the proton transfer event. The values of $\Delta\chi_4$ shows that the extent and direction of reorientation of Asn67 sidechain may be important in slowing down an ultrafast transfer of proton.

System 2

We have also presented below how the dynamical variations of these dihedral angles reflect changes in the system environment in System 2. Unlike in System 1, the short segments are of length 0.2 ps centered around the time of entry/exit to/from the barrier region. Comparison of Tables 2 (i) and (ii) indicates how these dihedral angles through their transient reorientations cooperatively facilitate the system in crossing the free energy barrier.

Table S3 The percentage change, $\Delta\chi$ of important active site dihedral angles obtained by averaging over the 0.2 ps segments extracted from transition paths belonging to the groups A, C, D and E in System 2.

(i) **Entrance to the free energy barrier region**

Group	$\Delta\chi_1$	$\Delta\chi_2$	$\Delta\chi_3$	$\Delta\chi_4$	$\Delta\chi_5$	$\Delta\chi_6$	$\Delta\chi_7$
A	-235.1	-4.8	-89.6	1321.8	-136.9	-1.4	-32.5
C	-242.0	4.2	-165.3	1512.7	-104.7	-32.2	-11.6
D	-239.2	6.3	-170.7	1470.4	-105.0	-10.2	-7.0
E	-237.0	7.7	-181.6	1440.2	-85.3	-16.7	-12.7

(ii) **Exit from the free energy barrier region**

Group	$\Delta\chi_1$	$\Delta\chi_2$	$\Delta\chi_3$	$\Delta\chi_4$	$\Delta\chi_5$	$\Delta\chi_6$	$\Delta\chi_7$
A	-225.7	-10.4	-93.5	1368.7	-112.7	-2.8	-33.3
C	-239.1	3.5	-162.4	1503.4	-92.4	-11.9	-10.0
D	-240.6	8.3	-171.3	1460.4	-104.6	-32.1	-6.7
E	-230.4	0.3	-171.7	1499.0	-100.4	-14.0	-0.3

- Roy, A.; Taraphder, S. Identification of Proton-Transfer Pathways in Human Carbonic Anhydrase Ii. *Journal of Physical Chemistry B* **2007**, *111*, 10563-10576.
- Maupin, C. M.; Voth, G. A. Preferred Orientations of His64 in Human Carbonic Anhydrase Ii. *Biochemistry* **2007**, *46*, 2938-2947.
- Basner, J. E.; Schwartz, S. D. How Enzyme Dynamics Helps Catalyze a Reaction in Atomic Detail: A Transition Path Sampling Study. *Journal of the American Chemical Society* **2005**, *127*, 13822-13831.
- Saen-Oon, S.; Schramm, V. L.; Schwartz, S. D. Transition Path Sampling Study of the Reaction Catalyzed by Purine Nucleoside Phosphorylase. *Zeitschrift Fur Physikalische Chemie-International Journal of Research in Physical Chemistry & Chemical Physics* **2008**, *222*, 1359-1374.
- Schwartz, S. D.; Schramm, V. L. Enzymatic Transition States and Dynamic Motion in Barrier Crossing. *Nature Chemical Biology* **2009**, *5*, 552-559.
- Best, R. B.; Hummer, G. Reaction Coordinates and Rates from Transition Paths. *Proceedings of the National Academy of Sciences of the United States of America* **2005**, *102*, 6732-6737.
- Rosta, E.; Woodcock, H. L.; Brooks, B. R.; Hummer, G. Artificial Reaction Coordinate "Tunneling" in Free-Energy Calculations: The Catalytic Reaction of Rnase H. *Journal of Computational Chemistry* **2009**, *30*, 1634-1641.
- Maupin, C. M.; Mckenna, R.; Silverman, D. N.; Voth, G. A. Elucidation of the Proton Transport Mechanism in Human Carbonic Anhydrase Ii. *Journal of the American Chemical Society* **2009**, *131*, 7598-7608.